Research Article | Vol. 26, No. 4 | 19 Feb 2018 | OPTICS EXPRESS 4440
Optics EXPRESS

Highly efficient nanosecond 560 nm source by SHG of a combined Yb-Raman fiber amplifier

T. H. Runcorn,* R. T. Murray, and J. R. Taylor

Femtosecond Optics Group, Department of Physics, Imperial College London, Prince Consort Road, London, SW7 2BW, UK
timothy.runcorn07@imperial.ac.uk

Abstract: We demonstrate a nanosecond 560 nm pulse source based on frequency-doubling the output of a combined Yb-Raman fiber amplifier, achieving a pulse energy of 2.0 μJ with a conversion efficiency of 32% from the 976 nm pump light. By introducing a continuous-wave 1120 nm signal before the cladding pumped amplifier of a pulsed Yb:fiber master oscillator power amplifier system operating at 1064 nm, efficient conversion to 1120 nm occurs within the fiber amplifier due to stimulated Raman scattering. The output of the combined Yb-Raman amplifier is frequency-doubled to 560 nm using a periodically poled lithium tantalate crystal with a conversion efficiency of 47%, resulting in an average power of 3.0 W at a repetition rate of 1.5 MHz. The 560 nm pulse duration of 1.7 ns and the near diffraction-limited beam quality ($M^2 \leq 1.18$) make this source ideally suited to biomedical imaging applications such as optical-resolution photoacoustic microscopy and stimulated emission depletion microscopy.

Published by The Optical Society under the terms of the Creative Commons Attribution 4.0 License. Further distribution of this work must maintain attribution to the author(s) and the published article's title, journal citation, and DOI.

OCIS codes: (140.3515) Lasers, frequency doubled; (140.3550) Lasers, Raman; (190.4370) Nonlinear optics, fibers.

References and links

1. K. Maslov, H. F. Zhang, S. Hu, and L. V. Wang, "Optical-resolution photoacoustic microscopy for *in vivo* imaging of single capillaries," Opt. Lett. **33**, 929–931 (2008).
2. S. W. Hell and J. Wichmann, "Breaking the diffraction resolution limit by stimulated emission: stimulated-emission-depletion fluorescence microscopy," Opt. Lett. **19**, 780–782 (1994).
3. D. Wildanger, E. Rittweger, L. Kastrup, and S. W. Hell, "STED microscopy with a supercontinuum laser source," Opt. Express **16**, 9614–9621 (2008).
4. P. Dupriez, C. Farrell, M. Ibsen, J. K. Sahu, J. Kim, C. Codemard, Y. Jeong, D. J. Richardson, and J. Nilsson, "1 W average power at 589 nm from a frequency doubled pulsed Raman fiber MOPA system," Proc. SPIE **6102**, 61021G (2006).
5. B. R. Rankin and S. W. Hell, "STED microscopy with a MHz pulsed stimulated-Raman-scattering source," Opt. Express **17**, 15679–15684 (2009).
6. E. E. Rowen, G. Vashdi, J. Lasri, and E. Inbar, "A scalable high-power yellow laser source based on frequency doubling of a combined Yb-Raman fiber amplifier," Proc. SPIE **8961**, 89611P (2014).
7. T. H. Runcorn, R. T. Murray, E. J. R. Kelleher, S. V. Popov, and J. R. Taylor, "Duration-tunable picosecond source at 560 nm with watt-level average power," Opt. Lett. **40**, 3085–3088 (2015).
8. T. H. Runcorn, T. Legg, R. T. Murray, E. J. R. Kelleher, S. V. Popov, and J. R. Taylor, "Fiber-integrated frequency-doubling of a picosecond Raman laser to 560 nm," Opt. Express **23**, 15728–15733 (2015).
9. A. Avdokhin, V. Gapontsev, P. Kadwani, A. Vaupel, I. Samartsev, N. Platonov, A. Yusim, and D. Myasnikov, "High average power quasi-CW single-mode green and UV fiber lasers," Proc. SPIE **9347**, 934704 (2015).
10. T. H. Runcorn, R. T. Murray, E. J. R. Kelleher, and J. R. Taylor, "Watt-level Nanosecond 589 nm Source by SHG of a Cascaded Raman Amplifier," in Lasers Congress 2016 (ASSL, LSC, LAC), OSA Technical Digest (online) (Optical Society of America, 2016), paper ATh1A.3.
11. L. Xu, S. Alam, Q. Kang, D. P. Shepherd, and D. J. Richardson, "Raman-shifted wavelength-selectable pulsed fiber laser with high repetition rate and high pulse energy in the visible," Opt. Express **25**, 351–356 (2017).
12. T. H. Runcorn, F. G. Görlitz, R. T. Murray, and E. J. R. Kelleher, "Visible Raman-shifted Fiber Lasers for Biophotonic Applications," IEEE J. Sel. Top. Quantum Electron. **24**, 1–8 (2018).
13. M. Dyba and S. W. Hell, "Photostability of a fluorescent marker under pulsed excited-state depletion through stimulated emission," Appl. Opt. **42**, 5123–5129 (2003).
14. T. H. Runcorn, R. T. Murray, and J. R. Taylor, "Microjoule Nanosecond 560 nm Source by SHG of a Combined Yb-Raman Fiber Amplifier," in Laser Congress 2017 (ASSL, LAC), OSA Technical Digest (online) (Optical Society of America, 2017), paper ATu1A.7.

#314840 https://doi.org/10.1364/OE.26.004440
Journal © 2018 Received 7 Dec 2017; revised 2 Feb 2018; accepted 2 Feb 2018; published 12 Feb 2018

Optics EXPRESS

15. M. Nakamura, S. Takekawa, K. Terabe, K. Kitamura, T. Usami, K. Nakamura, H. Ito, and Y. Furukawa, "Near-stoichiometric LiTaO3 for bulk quasi-phasematched devices," Ferroelectrics **273**, 199–204 (2002).
16. M. Eibl, S. Karpf, H. Hakert, T. Blömker, J. P. Kolb, C. Jirauschek, and R. Huber, "Pulse-to-pulse wavelength switching of a nanosecond fiber laser by four-wave mixing seeded stimulated Raman amplification," Opt. Lett. **42**, 4406–4409 (2017).
17. S. M. Riecke, H. Wenzel, S. Schwertfeger, K. Lauritsen, K. Paschke, R. Erdmann, and G. Erbert, "Picosecond Spectral Dynamics of Gain-Switched DFB Lasers," IEEE J. Quantum Electron. **47**, 715–722 (2011).

1. Introduction

Laser sources operating in the yellow-green spectral region (550–600 nm) are required for a variety of biomedical imaging applications such as optical-resolution photoacoustic microscopy (OR-PAM) [1] and stimulated emission depletion (STED) microscopy [2]. For OR-PAM, nanosecond pulses with microjoule-level pulse energy are advantageous to maximize the ultrasound signal to noise ratio whilst adhering to laser safety standards. In STED microscopy, a depletion beam pulse duration in the range 0.1–2 ns [3] provides the best resolution improvement over confocal microscopy whilst minimizing the average power required (important for live cell imaging) in comparison to continuous-wave (CW) depletion. For both techniques, megahertz pulse repetition rates are desirable to obtain fast image acquisition times and near diffraction-limited beam quality enables the best possible optical resolution to be achieved.

Over the last decade, the use of stimulated Raman scattering (SRS) in combination with second-harmonic generation (SHG) has been demonstrated as an effective route to accessing the yellow-green spectral region using pulsed Yb:fiber master oscillator power amplifier (MOPA) systems [4–11]. The order in which the nonlinear conversion processes are performed and the architecture employed has a significant impact on the practical aspects of the sources, which we recently reviewed in detail [12]. Arguably the most conceptually straightforward approach is to use cascaded SRS in a passive optical fiber to efficiently frequency downshift the output of a frequency-doubled Yb:fiber MOPA system [5, 11]. This technique has great wavelength flexibility but the need to couple high intensity green light into an optical fiber introduces sensitive optical alignment and raises questions about the long-term reliability due to photoinduced damage. These issues can be avoided by frequency-doubling a Raman-shifted Yb:fiber MOPA system, however, to achieve high SHG conversion efficiencies, techniques to reduce the spectral bandwidth of the Raman-shifted light must be implemented [6–10]. Seeding the SRS process with a narrow linewidth CW signal at the Raman-shifted wavelength is a convenient method of achieving this, since the temporal properties of the Raman-shifted light are predominantly determined by the master oscillator pulses [6–8, 10].

In a combined Yb-Raman fiber amplifier system, the CW seed signal at the Raman-shifted wavelength is multiplexed with pulses in the Yb:fiber gain band before the final fiber power amplifier stage [4, 6]. If the amplifier fiber characteristics (length, mode field diameter) and the pulse parameters are chosen correctly, power will be efficiently transferred by SRS from the amplified pulses to the Raman-shifted wavelength within the amplifier fiber. The output of these combined Yb-Raman fiber amplifiers can then be directly frequency-doubled into the yellow-green spectral region [4, 6]. Using this architecture, Rowen *et al.* achieved a 565 nm pulse energy of 11.3 μJ at a repetition rate of 2 MHz with a conversion efficiency of 26% from the 915 nm combined Yb-Raman fiber amplifier pump power [6]. In their demonstration, efficient Raman conversion required a pulse peak-power of ~10 kW due to the use of a large mode area Yb-doped fiber for the combined Yb-Raman amplifier. For STED microscopy, it is desirable to use the lowest peak-power possible to avoid photobleaching and photodamage of the sample, since these are multiphoton processes [13]. In this contribution, we achieve a higher pump-to-visible conversion efficiency with a lower pulse peak-power by using a periodically poled lithium tantalate crystal to frequency-double the output of a single-mode combined Yb-Raman fiber amplifier, expanding on the work presented in [14]. We generate a 560 nm average power of

Optics EXPRESS

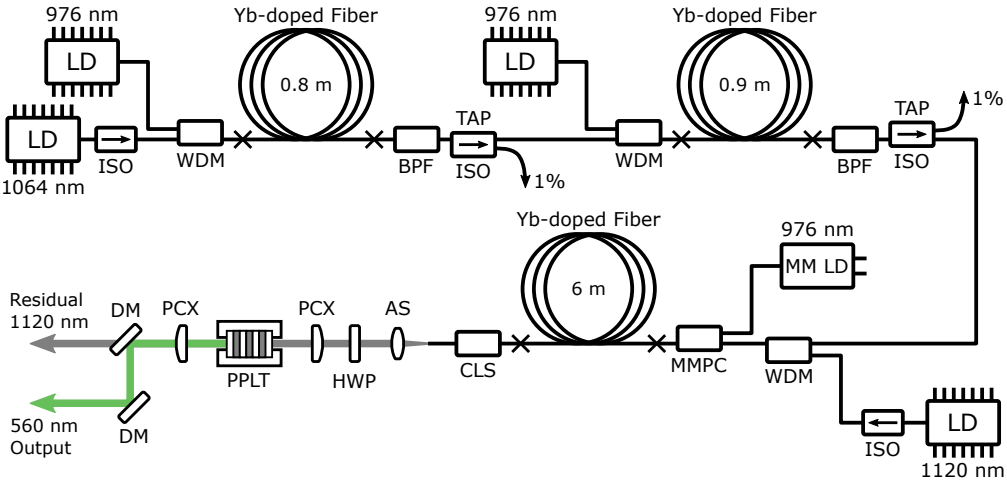


Fig. 1. Schematic of the frequency-doubled combined Yb-Raman amplifier system. LD, laser diode; ISO, optical isolator; WDM, wavelength division multiplexer; BPF, bandpass filter; TAP, tap coupler; MM LD, multimode laser diode; MMPC, multimode pump combiner; CLS, cladding light stripper; AS, aspheric lens; HWP, half waveplate; PCX, plano-convex lens; PPLT, periodically poled lithium tantalate; DM, dichroic mirror.

3.0 W with a conversion efficiency of 32% from the 976 nm combined Yb-Raman fiber amplifier pump power, which to the best of our knowledge is the highest reported conversion efficiency for a frequency-doubled combined Yb-Raman fiber amplifier system to date.

2. Experimental setup

The schematic of the nanosecond 560 nm source based on frequency-doubling the output of a combined Yb-Raman fiber amplifier is shown in Fig. 1. A distributed feedback (DFB) laser diode operating at 1064 nm (QD Laser QLD1061) was pulsed using a duration-tunable electrical pulse generator to generate the nanosecond-duration optical seed pulses. The seed pulses were pre-amplified using two single-mode Yb-doped fiber (Liekki Yb1200-6/125DC-PM) amplifier stages, core-pumped by 976 nm fiber Bragg grating (FBG) stabilized laser diodes (Thorlabs BL976-PAG500) via filter-type wavelength division multiplexers (WDM). Bandpass filters with a 2 nm pass band (0.5 dB level) at 1064 nm were used after each stage to eliminate the amplified spontaneous emission generated at shorter wavelengths. A hybrid optical isolator and tap coupler device was used after each pre-amplifier stage to monitor the seed power and prevent the amplification of backwards propagating light. Before the cladding pumped power amplifier stage, a narrow linewidth CW signal at 1120 nm from a FBG-stabilized laser diode (Innolume LD-1120-FBG-400) was combined with the pre-amplified seed pulses using a filter-type WDM.

The power amplifier stage ultilized a 6 m length of single-mode Yb-doped fiber (Liekki Yb1200-6/125DC-PM), cladding pumped by a wavelength-stabilized 976 nm multimode pump diode (BWT K976A02RN-9.000W) via a multimode pump combiner. A 0.8 m length of PM980 fiber was spliced to the output of the amplifier and the splice was recoated in high-index acrylate to strip any unabsorbed pump light from the cladding. The output of the PM980 fiber was angle cleaved to inhibit feedback from the Fresnel backreflection and collimated using an antireflection (AR) coated aspheric lens. All of the fibers used in the combined Yb-Raman amplifier system were polarization maintaining, which ensured that the linear polarization of the 1064 nm and 1120 nm laser diodes was preserved and that the system was robust against environmental perturbations.

Optics EXPRESS

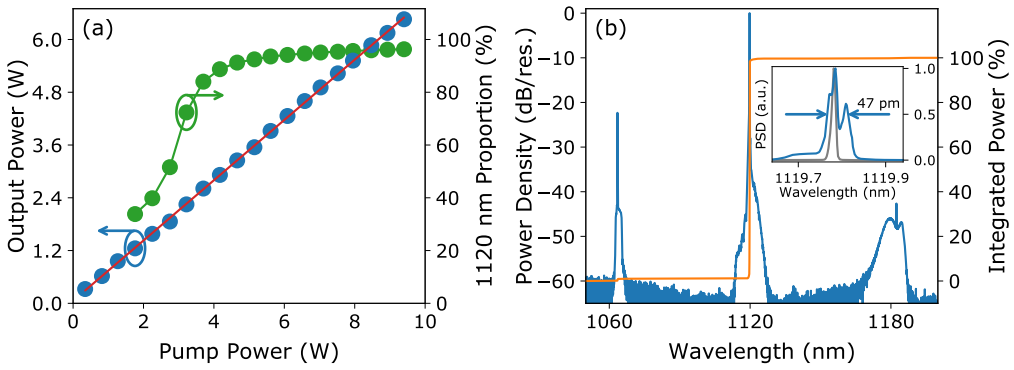


Fig. 2. (a) Combined Yb-Raman amplifier output power (blue points) and 1120 nm amplified pulse proportion (green points) as a function of 976 nm pump power with a linear regression (red line) revealing a slope efficiency of 69%. Green line is a guide for the eye. (b) Optical spectrum (blue line) of the amplifier output at a pump power of 9.4 W with the integrated spectral power (orange line). Inset: optical spectrum of the 1120 nm seed (gray line) and amplifier output (blue line).

A 20 mm long periodically poled lithium tantalate (PPLT) crystal (HC Photonics) was used to frequency-double the output of the combined Yb-Raman fiber amplifier. The PPLT crystal was poled with a single 9.12 µm pitch grating for quasi phase-matching SHG of 1120 nm at a temperature of ~115°C with a corresponding 3 dB spectral acceptance bandwidth of 0.15 nm in the low pump depletion regime. The crystal had an aperture of 1×0.5 mm^2 and was AR-coated for 1120 nm (R<0.3%) and 560 nm (R<0.5%) on the input and output facets. To increase the photorefractive damage threshold, the crystal had a stoichiometric composition and was doped with 1 mol.% MgO [15]. A half waveplate was used to align the linear output polarization of the combined Yb-Raman fiber amplifier to the z axis of the PPLT crystal to utilize type-0 (all waves extraordinary polarized) phase-matching. The output of the combined Yb-Raman fiber amplifier was focused to a $1/e^2$ beam diameter of 83 µm in the PPLT crystal, corresponding to a focusing parameter of $\xi = L/b = 1.0$, where L is the crystal length and b is the confocal parameter of the fundamental beam in the crystal. A plano-convex lens was used to collimate the generated second-harmonic, which was subsequently separated from the residual fundamental using two longpass dichroic mirrors (Thorlabs DMLP950).

3. Experimental results and discussion

3.1. Combined Yb-Raman fiber amplifier

The electrical pulse generator of the 1064 nm laser diode was set to generate optical pulses with a duration of ~2 ns, the longest duration suitable for STED microscopy, in order to maximize the demonstrated 560 nm pulse energy. This duration was also chosen to increase the threshold of deleterious stimulated Brillouin scattering beyond the SRS threshold, which would otherwise be an issue due to the narrow spectral linewidth of the 1064 nm DFB laser diode. It is worth noting that broader spectral bandwidth sources, such as Fabry-Pérot laser diodes or mode-locked fiber oscillators, have been demonstrated as equally effective pulse sources [6, 8]. At a pulse repetition rate of 1.5 MHz, the 1064 nm laser diode delivered a pulse energy of 107 pJ, which was amplified to 30 nJ after the two pre-amplifier stages using a pump power of 200 mW for the first stage and 300 mW for the second stage. The 1120 nm laser diode was operated at a drive current of 500 mA, which corresponded to a CW signal power of 160 mW at the input of the active fiber. All of the experimental results that follow used these 1064 nm pulse and 1120 nm

Optics EXPRESS

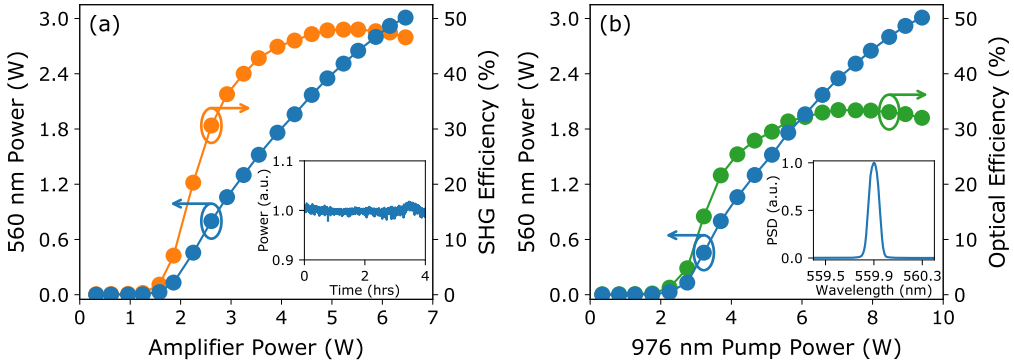


Fig. 3. (a) Second-harmonic average power at 560 nm (blue points) and conversion efficiency (orange points) as a function of combined Yb-Raman fiber amplifier output power. Inset: 560 nm average power stability. (b) Second-harmonic average power at 560 nm (blue points) and optical efficiency (green points) as a function of 976 nm amplifier pump power. Inset: optical spectrum of the second-harmonic. Lines are a guide for the eye.

CW parameters.

Figure 2(a) shows the average output power of the combined Yb-Raman fiber amplifier (blue points) as a function of 976 nm pump power, a linear relationship is evident (red line), corresponding to a slope efficiency of 69%. At the maximum available pump power of 9.40 W, the average output power of the combined Yb-Raman fiber amplifier was 6.46 W. No saturation of the output power was evident, suggesting that the efficiency of the combined Yb-Raman fiber amplifier could be maintained at higher pump powers if the repetition rate of the signal pulses and the input power were increased proportionally.

A longpass dichroic mirror with a cut-on wavelength of 1100 nm that had an attenuation of 40 dB for wavelengths shorter than 1080 nm was used to determine the proportion of the amplifier output that was the amplified 1120 nm signal [green points Fig. 2(a)]. Since the Raman gain is only available in the window of the 1064 nm pulses, the average power at 1120 nm was comprised of amplified pulses and the CW seed signal between the pulses. To give a more accurate reflection of the proportion of the amplifier output that is the amplified 1120 nm pulses, therefore, the CW signal power was subtracted in the 1120 nm proportion presented in Fig. 2(a). Over the pump power range 7.0–9.4 W, greater than 95% of the amplifier output was the amplified 1120 nm pulses, demonstrating excellent conversion from 1064 nm to 1120 nm in the amplifier.

Figure 2(b) shows the optical spectrum of the combined Yb-Raman fiber amplifier output at the maximum pump power of 9.4 W. The integrated spectral power [orange line Fig. 2(b)] corroborates the average power measurements taken with the longpass filter and demonstrates the high power spectral density of the amplified 1120 nm signal. It is worth noting, however, that the level of the 1120 nm peak includes the CW seed signal that is present between the pulses. The 3 dB spectral bandwidth of amplified 1120 nm signal was 47 pm, which was broadened from the seed linewidth (<10 pm, limited by the resolution of the optical spectrum analyzer) due to cross and self-phase modulation in the combined Yb-Raman fiber amplifier [inset Fig. 2(b)].

Amplified spontaneous Raman scattering at the second Stokes shift around 1180 nm is evident in Fig. 2(b), highlighting the potential to extend the wavelength coverage of this architecture [10, 16]. The narrow peak seen at 1182 nm in Fig. 2(b) was generated by four-wave mixing between the 1064 nm seed pulses and the 1120 nm amplified signal, as evidenced by the equal 14.2 THz frequency spacing. This has previously been observed in combined Yb-Raman fiber amplifier systems and provides a mechanism to reduce the spectral bandwidth of the light at the second Stokes shift without having to provide a narrow linewidth signal [16].

Optics EXPRESS

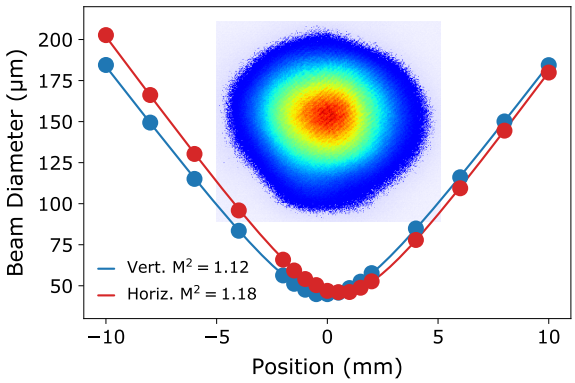


Fig. 4. 560 nm beam quality measurement based on a Gaussian beam caustic fit (lines) to the measured beam diameter (points) through the focus of a lens. Inset: CCD camera image of the collimated 560 nm beam.

3.2. *Frequency-doubling to 560 nm*

The high power spectral density, linearly polarized output (polarization extinction ratio of 23 dB) of the combined Yb-Raman amplifier had ideal parameters for efficient SHG using the 20 mm long PPLT crystal. Figure 3(a) shows the generated 560 nm second-harmonic average power and conversion efficiency as a function of the combined Yb-Raman fiber amplifier output power. A maximum 560 nm average power of 3.01 W was generated for an amplifier output power of 6.46 W, corresponding to a conversion efficiency of 47%. This conversion efficiency is a slight underestimate of the actual SHG conversion efficiency due to small (<1.5%) residual 1064 nm power and the presence of the CW 1120 nm seed power between pulses, which is poorly converted. To confirm this, the 1120 nm CW seed signal of 160 mW was frequency-doubled when the combined Yb-Raman amplifier was not pumped and not seeded with 1064 nm pulses and ~30 μW of 560 nm average power was generated. This implies, therefore, that the 560 nm pulses have a temporal contrast of ~50 dB from the continuous background, justifying the use of a CW 1120 nm seed signal. Without any active current stabilization, the 560 nm average power of 3.0 W had a power stability of <0.5% rms over four hours [inset Fig. 3(a)], which was mainly limited by changes in the ambient conditions since the fiber and fiber components were not actively temperature stabilized.

Figure 3(b) shows the generated 560 nm average power as a function of the 976 nm amplifier pump power with the corresponding overall optical efficiency. At the maximum available 976 nm pump power of 9.40 W, the overall conversion efficiency to 560 nm was 32%. This conversion efficiency was slightly less than the maximum, which exceeded 33%, due to a slight roll-off in the SHG conversion efficiency [Fig. 3(a)]. The roll-off in the SHG conversion efficiency was caused by the monotonically increasing spectral bandwidth of the amplified 1120 nm signal with amplifier pump power due to nonlinear effects in the combined Yb-Raman amplifier [inset Fig. 2(b)]. It is worth noting that the pump power at which the maximum conversion efficiency occurs could easily be shifted to the maximum available pump power by increasing the repetition rate of the 1064 nm seed pulses. The 3 dB spectral bandwidth of the 560 nm light was <0.1 nm, limited by the resolution of the optical spectrum analyzer [inset Fig. 3(b)].

To measure the 560 nm beam quality at the maximum average power, a pyroelectric scanning slit beam profiler was used to measure the 4σ beam diameter through the focus of an f=75 mm plano-convex lens. Figure 4 shows the measured beam diameters (points) with a Gaussian fit to the beam caustics (lines), which revealed an M^2=1.12 and M^2=1.18 in the vertical and horizontal axes, respectively. The inset of Fig. 4 shows a CCD camera image of the collimated 560 nm

Optics EXPRESS

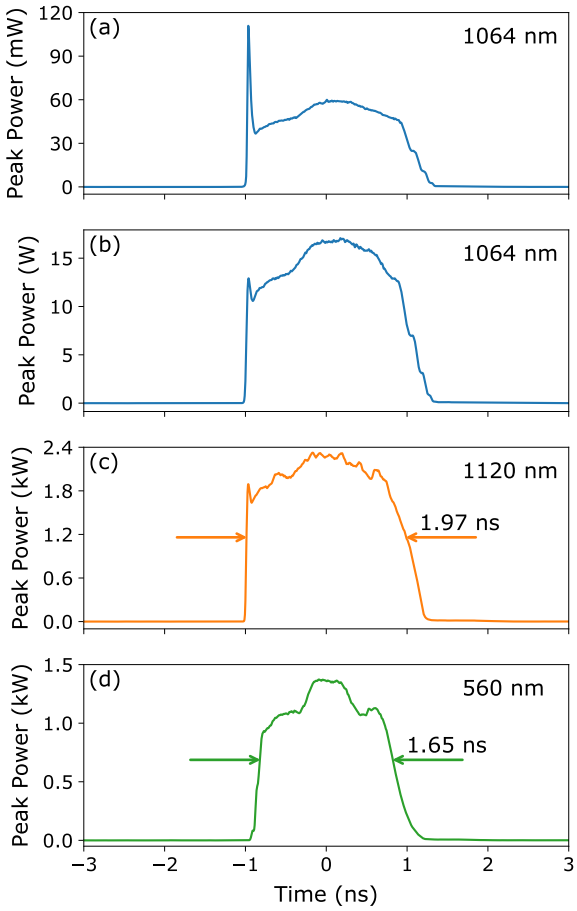


Fig. 5. Sampling optical oscilloscope traces of the 1064 nm laser diode seed pulses (a), 1064 nm pulses at the second pre-amplifier tap (b), filtered 1120 nm amplifier output at maximum pump power (c) and the frequency-doubled pulses (d) at a pulse repetition rate of 1.5 MHz.

beam, which had an ellipticity of 0.9.

Figure 5 shows the evolution of the optical pulses through the frequency-doubled combined Yb-Raman fiber amplifier system, measured using a sampling optical oscilloscope (Hamamatsu OOS-01) with a rise time of ≤20 ps. The generated 1064 nm seed pulses are typical of those from a directly modulated DFB laser diode [17], comprised of a short (~50 ps) fixed duration relaxation oscillation followed by a longer tail [Fig. 5(a)], the duration of which can be tuned by adjusting the duration of the electrical drive pulse. The measured peak-power of the relaxation oscillation feature relative to the tail decreases after the two pre-amplifiers [Fig. 5(b)], the cause of which is currently under investigation, and this shape is transferred to the 1120 nm pulses in the Raman conversion [Fig. 5(c)]. The frequency-doubled 560 nm pulse duration of 1.65 ns [Fig. 5(d)] is shortened from the fundamental 1120 nm pulse duration due to nonlinear relationship between the SHG conversion efficiency and the instantaneous pulse peak-power. This pulse duration is well suited to photoacoustic microscopy and fluorescence-based imaging techniques such as STED microscopy [1, 3].

Optics EXPRESS

4. Conclusion

In conclusion, we have demonstrated a highly efficient architecture for generating nanosecond-duration pulses in the strategically important yellow-green (550–600 nm) spectral region based on frequency-doubling the output of a combined Yb-Raman fiber amplifier in a periodically poled crystal. We generated a 560 nm average power of 3.0 W when the fiber amplifier was pumped with 9.4 W of 976 nm multimode diode power, corresponding to an overall conversion efficiency of 32%. To the best of our knowledge, this is the highest reported pump to yellow-green light conversion efficiency for a frequency-doubled combined Yb-Raman system to date. The 560 nm pulse energy of 2.0 μJ with a pulse duration of 1.7 ns and near diffraction-limited beam quality mean that this compact, turn-key source should find applications in biomedical imaging applications such as OR-PAM and STED microscopy.

Funding

Engineering and Physical Sciences Research Council (EPSRC) (EP/N009452/1, EP/K503733/1); Medical Research Council (MRC) (MR/K015834/1); The European Office of Aerospace Research and Development (EOARD) (FA9550-17-1-0194); THR was supported by an EPSRC Doctoral Prize Fellowship.

Acknowledgments

The authors would like to thank P. M. W. French and C. Dunsby for engaging discussions. The data used in this paper is openly available at: https://doi.org/10.5281/zenodo.1166082.

155.198.12.188 {ts '2018-03-28 04:10:09'}